CMS Physics Analysis Summary

Contact: cms-pag-conveners-bphysics@cern.ch 2009/07/29

Feasibility study of a J/ψ cross section measurement with early CMS data

The CMS Collaboration

Abstract

We report on the methods and plans for measuring the differential p_T $J/\psi \to \mu^+\mu^-$ production cross section, using data to be collected in the first LHC run by the CMS detector. Making use of the large B-hadron lifetime, we show how to separate the promptly produced J/ψ's from those coming from B-hadron decays. Since the J/ψ production cross section is expected to be large, the analysis should be viable with relatively small data sets, that will become available early in the startup of the LHC. We also address effects of a non-perfect detector alignment, as well as systematic uncertainties.

About 70 thousand J/ψ decays are reconstructed for an integrated luminosity of 3 pb^{-1} in 14 TeV collisions, in the range of $p_T^{J/\psi}$ between 5 and 40 GeV/c. The precision of the result is limited by systematic uncertainties, and is at the 15 % level.

1 Introduction

Three processes dominate J/ψ hadro-production: prompt J/ψ's produced directly, prompt J/ψ's produced indirectly (via decay of heavier charmonium states such as χ_c), and non-prompt J/ψ's from the decay of a B-hadron. It is the prompt production of quarkonia which continues to be particularly puzzling. There are a variety of production models available for prompt quarkonium production [1–3], among which are the *Colour Singlet Model* (CSM) and the *Colour Octet Mechanism* (COM). The latter owes its popularity to the fact that it is able to reproduce the CDF J/ψ differential-p_T cross section data [3–5]. However, the polarization predictions of the COM are in strong disagreement with measurements [6, 7]. In view of the puzzling situation, and given the large yields of quarkonia which will be produced at the LHC, the early data collected by CMS present an excellent opportunity to study quarkonia. The measurement is expected not to be limited by statistics, but rather by the limited knowledge of the CMS detector, especially at startup. The precision tracking permits us to disentangle the prompt J/ψ production from that coming from B-hadron decays, and therefore allows usto determine the B-hadron cross section. Already with the small integrated luminosity foreseen to be delivered by the LHC during the 2008 run, it is possible to obtain a result competitive to the Tevatron measurements over the J/ψ transverse momenta of from about 5 GeV/c up to about 40 GeV/c.Eventually, thanks to the much higher collision energy and luminosity, the studies of quarkonia with CMS will probe much higher momentum values, extending the test of the different production mechanisms in regions never probed before. In addition CMS offers a larger pseudorapidity coverage than that of the Tevatron experiments, giving the possibility to study other dependencies.

In this note we describe the measurement of the $J/\psi \rightarrow \mu^+\mu^-$ differential cross section as a function of $p_T^{J/\psi}$, with 3 pb^{-1} of data collected at a centre-of-mass energy of 14 TeV. Contributions from prompt and non-prompt J/ψ's will be separated by using lifetime distributions. In the following we discuss event generation, trigger issues, muon and J/ψ reconstruction, and the measurement of the prompt and the non-prompt J/ψ p_T differential cross sections. Misalignment effects and systematic uncertainties on the measurement are also addressed.

2 Event generation and Monte-Carlo samples

Events containing prompt J/ψ's were produced using Pythia 6.409 [8], which generates events based on the leading-order singlet and octet mechanisms. Colour octet states undergo a shower evolution. We used the NRQCD matrix element tuning as was obtained by comparing NRQCD calculations with CDF data [3, 9]. The polarization during event generation was set to zero. Events containing non-prompt J/ψ's from B-hadron decays were generated by using the generic QCD 2$\rightarrow$2 event generation in Pythia (MSEL=1). All J/ψ events were generated requiring the J/ψ to be produced with $|\eta^{J/\psi}| < 2.5$ and both decay muons to have $p_T^{\mu} > 2.0$ GeV/c and $|\eta^{\mu}| < 2.5$.

As background events we have considered any other source of muons that, when paired, could accidentally have an invariant mass close to that of the J/ψ. The following sources of background events were considered:

- generic QCD 2$\rightarrow$2 events produced with Pythia (MSEL=1), requiring the presence of one μ with $p_T^{\mu} > 2.5$ GeV/c and $|\eta^{\mu}| < 2.5$ at generator level, mainly coming from D and B meson decays. These events are referred to as "muon enriched QCD background" in the following. This background sample takes into account combinations of two muons from different origins except the case where both muons would be

due to pion or kaon decays. Neglecting this background contribution has a small effect in our results and will be considered as a contribution to the systematic uncertainties.

- Drell-Yan events where both muons have $p_T^\mu > 2.0$ GeV/c and $|\eta^\mu| < 2.5$.

Overall, about 2 million prompt J/ψ events, 1 million B-hadron decay events, 2 million Drell-Yan and 20 million muon-enriched minimum-bias events were produced, processed through a full GEANT based detector simulation, and passed through the standard CMS reconstruction program.

3 J/ψ trigger selection

The J/ψ trigger is described in Ref. [10]. It consists of a Level1 trigger (L1), based on the muon chamber information, followed by a High Level Trigger (HLT) step, that confirms the L1 and refines the reconstruction adding the silicon tracker information. The L1 is based on the request of two muons each with $p_T^\mu > 3$ GeV/c as measured in the muon stations, while the HLT step recomputes the p_T^μ with better precision, requiring it to be larger than 3 GeV/c and that the invariant mass of the reconstructed muon pair lies between 2.8 and 3.4 GeV/c^2. The trigger rates after the full trigger chain (L1 followed by the HLT) at an instantaneous luminosity of 10^{32} cm^{-2}s^{-1} are shown in Table 1, together with the number of events N expected to be triggered in a sample with an integrated luminosity of 3 pb^{-1}.

Table 1: Combined L1+HLT J/ψ trigger rates at an instantaneous luminosity of 10^{32} cm^{-2}s^{-1} and the number of expected events N in 3 pb^{-1}.

	Trigger rate (Hz)	N
Prompt J/ψ	1.92	58K
B-decay J/ψ	0.85	26K
QCD background	0.40	12K

4 Muon and J/ψ reconstruction

Muon reconstruction is described in detail in Ref. [11]. Reconstruction makes use of the muon chambers and of the silicon tracker by first finding a segment in the muon stations, which is then matched to a compatible track in the silicon tracker. A combined fit of the muon segment and silicon tracks trajectory yields the final reconstructed muon track. The η-coverage for muon reconstruction in the CMS detector is $|\eta^\mu| < 2.4$. The muon reconstruction efficiency, defined as the ratio between the number of reconstructed muons and the number of generated muons, depends on p_T^μ and η^μ, and also takes into account the detector acceptance. For $|\eta^\mu| > 1.4$ the muon reconstruction efficiency is about 85% for muons with $p_T^\mu > 3$ GeV/c. For $|\eta^\mu| < 1.4$ the reconstruction efficiency drops dramatically for $p_T^\mu < 7$ GeV/c due to the ionization energy losses in the material before reaching the muon stations. The maximum efficiency, which is much more than 90%, is reached for $p_T^\mu > 7$ GeV/c, for all η^μ, except for a few inter-detector boundaries. The momentum resolution of the muons is at the percent level. Among the reconstructed muons that survive our selection criteria, only a very small fraction (around 0.3%) is due to decays of pions or kaons. Indeed, most of these muons fail to pass the p_T^μ cut or are rejected in the matching step between the track in the muon chambers and the track in the silicon layers.

J/ψ candidates are reconstructed by pairing muons with at least 3 GeV/c transverse momentum and opposite charge. The invariant mass of the muon pair is required to be between 2.8 and 3.4 GeV/c^2. The two muons are required to come from a common vertex, which is determined by the point of their closest approach in space. Since the dimuon mass resolution depends on the pseudorapidity (~ 17 MeV/c^2 at $\eta = 0$ and ~ 40 MeV/c^2 at $|\eta| = 2.4$), we used a double Gaussian to fit the simulated J/ψ signal. For the background continuum we used a linear function but the results remain the same if we use an exponential. The dimuon mass spectrum including background and signal is given in Fig. 1. The level of the Drell-Yan background in the same mass window, is computed to be less than than a percent with respect to the other background sources, and hence neglected from now on. In our event sample, muon pairs where both muons come from pion or kaon decays should occur at a rate around 10% of the "muon enriched QCD background" we have considered; it is taken into account as a systematic uncertainty

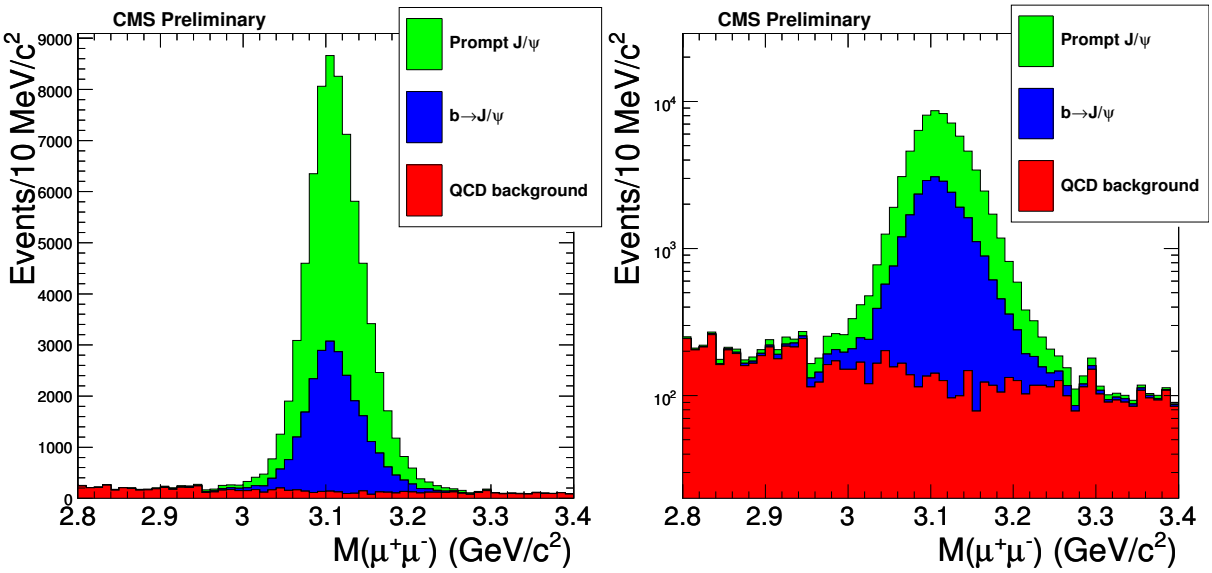

Figure 1: Dimuon invariant mass distribution normalized to 3 pb^{-1} in linear (left) and logarithmic (right) scale. The green (light grey), blue (black) and red (dark grey) areas are the prompt, non-prompt and QCD background contributions, respectively.

The resulting number of fitted events for the signal, divided by the total number of generated events, defines the signal reconstruction efficiency convoluted with acceptance, which depends on $p_T^{J/\psi}$, $\eta^{J/\psi}$ and on the J/ψ polarization. The reconstruction efficiency is given in Fig. 2, as function of $p_T^{J/\psi}$, for J/ψ produced with $|\eta^{J/\psi}| < 2.4$. This efficiency takes into account the finite acceptance of the detector and thus the plateaux in Fig. 2 are significantly lower than the intrinsic efficiency for high p_T muons of about 95-99% [11].

5 Measurement of prompt and non-prompt J/ψ cross sections

5.1 Inclusive measurement

The inclusive $p_T^{J/\psi}$ differential cross section measurement, covering the region $|\eta^{J/\psi}| <2.4$, is based on the following expression:

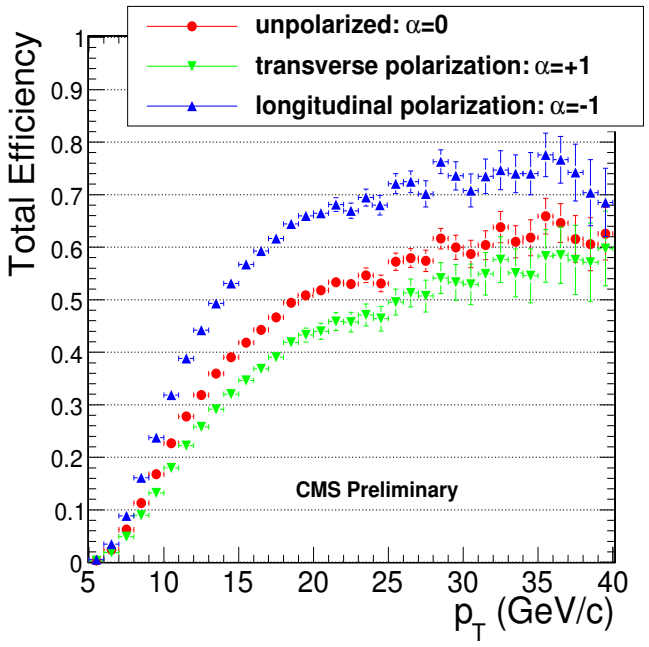

Figure 2: Efficiency convoluted with acceptance as a function of $p_T^{J/\psi}$, shown for three different polarizations of the J/ψ.

$$\frac{d\sigma}{dp_T}(J/\psi) \cdot Br(J/\psi \to \mu^+\mu^-) = \frac{N_{J/\psi}^{fit}}{\int Ldt \cdot A \cdot \lambda_{trigger}^{corr} \cdot \lambda_{reco}^{corr} \cdot \Delta p_T} \tag{1}$$

where

- $N_{J/\psi}^{fit}$ is the number of reconstructed J/ψ in a given p_T bin resulting from the mass spectrum fit, as explained in Section 4.
- Δp_T is the size of the p_T bin.
- $\int Ldt$ is the integrated luminosity.
- A is the total efficiency for triggering and reconstructing the J/ψ events, as extracted from Monte Carlo simulation, taking also into account the finite acceptance of the detector. This is shown in Fig. 2 as a function of $p_T^{J/\psi}$. As mentioned earlier, the value for the polarization in the Monte Carlo was set to zero, and the dependence of the acceptance on the polarization is treated as systematic effect.
- $\lambda_{trigger}^{corr}$ and λ_{reco}^{corr} are correction factors to the trigger and offline efficiencies, respectively, determined by comparing the measured distributions with those simulated by Monte Carlo. We will make use of the so called "tag and probe" methods to determine all corrections [12]. In this method one reconstructs a known resonance (for instance a Y) decaying into a muon pair, in single muon triggered events. As an example, in order to check the muon tracking reconstruction efficiency one fully reconstructs only one muon (the tag) while the other (the probe) is only required to be reconstructed with the muon chambers. The pair is required to have an invariant mass compatible with the resonance. By checking how many times the probe is reconstructed in the tracker one determines the tracking efficiency. This method can be applied to any reconstruction variable both in data and in Monte Carlo simulations, thus determining the λ correction factors.

5.2 Measurement of the J/ψ feed-down fraction from B decays

For each J/ψ candidate, we computed $\ell_{xy} = L_{xy} \cdot m_{J/\psi}/p_T^{J/\psi}$ where L_{xy} is the distance in the transverse plane between the vertex of the two muons (as defined in Section 4) and the primary vertex of the event, and $m_{J/\psi}$ is the J/ψ mass.

To determine the fraction f_B of J/ψ's from B-hadron decays, we performed an unbinned maximum-likelihood fit to the data. In analogy with the method used in Ref. [5], the dimuon mass spectrum and the ℓ_{xy} distribution were simultaneously fitted by a log-likelihood function L:

$$\ln L = \sum_{i=1}^{N} \ln F(\ell_{xy}, m_{\mu\mu}), \tag{2}$$

where N is the total number of events and $m_{\mu\mu}$ is the invariant mass of the muon pair. The expression for $F(\ell_{xy}, m_{\mu\mu})$ is given by:

$$F(\ell_{xy}, m_{\mu\mu}) = f_{Sig} \times F_{Sig}(\ell_{xy}) \times M_{Sig}(m_{\mu\mu}) + (1 - f_{Sig}) \times F_{Bkg}(\ell_{xy}) \times M_{Bkg}(m_{\mu\mu}) \tag{3}$$

where:

- f_{Sig} is the fraction of events attributed to J/ψ sources coming from both prompt and non-prompt components,
- $F_{Sig}(\ell_{xy})$ and $F_{Bkg}(\ell_{xy})$ are the functional forms describing the ℓ_{xy} distribution for the signal and background, respectively. The signal part is given by a sum of prompt and non-prompt components:

  $$F_{Sig}(\ell_{xy}) = f_B \times F_B(\ell_{xy}) + (1 - f_B) \times F_p(\ell_{xy}), \tag{4}$$

  where f_B is the fraction of J/ψ from B-hadron decays, and $F_p(\ell_{xy})$ and $F_B(\ell_{xy})$ are the ℓ_{xy} distributions for prompt and non-prompt J/ψ's respectively. $F_p(\ell_{xy})$ is described by a resolution function that is taken from the Monte Carlo reconstructed events, but that can be determined from the p-p collision data, once available. The ℓ_{xy} shape of the non-prompt component of Eq. 4 is given by the convolution of the same resolution function with the true ℓ_{xy} distribution of the J/ψ's from B-decays as coming from the Monte Carlo simulation.

  With regard to the background ℓ_{xy} distribution, $F_{Bkg}(\ell_{xy})$, we used the functional form that CDF employed in their analysis [5].
- $M_{Sig}(m_{\mu\mu})$ and $M_{Bkg}(m_{\mu\mu})$ are the functional forms describing the invariant dimuon mass distributions for the signal and background, respectively.

We divided the event sample in 15 $p_T^{J/\psi}$ bins (of at least 2000 reconstructed events each) and performed the unbinned likelihood fit in each of them. Figure 3 shows an example of the fit results in the region of $9 < p_T^{J/\psi} < 10$ GeV/c.

6 Effects due to residual misalignments

The alignment of the tracking detectors will be pursued with data, with increasing precision following the rise of the integrated luminosity. In order to understand any possible bias and degradations in the mass fit and in disentangling the prompt and non-prompt components due to residual misalignments, we have re-reconstructed the same samples in different misalignment scenarios [11], that represent the assumed precision of the alignment after some

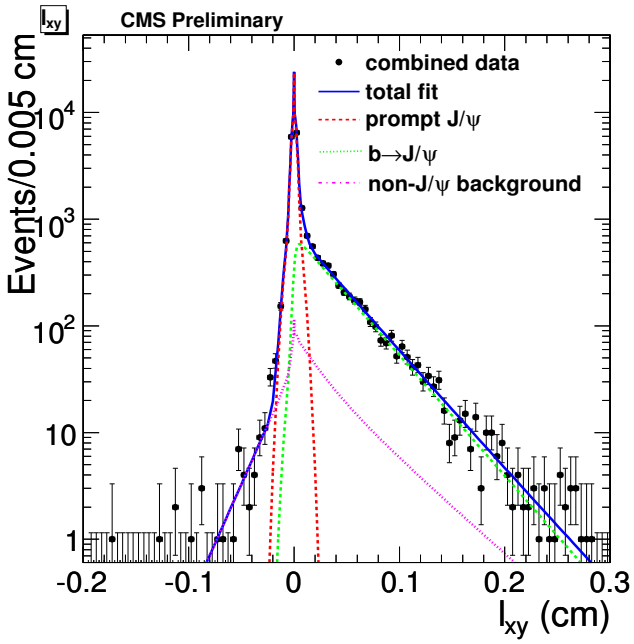

Figure 3: Distribution of ℓ_{xy} and likelihood fit result in the range of $9 < p_T < 10\,\mathrm{GeV}/c$.

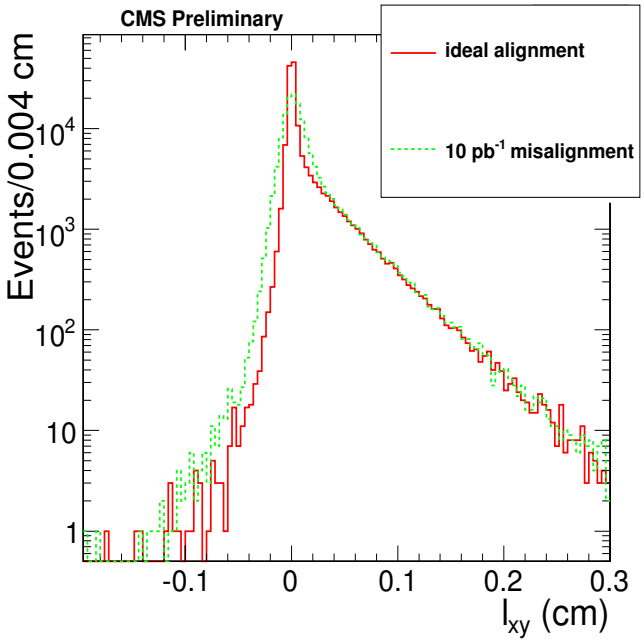

Figure 4: The ℓ_{xy} distribution for prompt and non-prompt J/ψ for different misalignment scenarios. The non-prompt J/ψ exponential tail is clearly visible and is almost insensitive to misalignment.

integrated luminosity. The effect of misalignment on the J/ψ mass resolution is shown in Table 2. The worse tracking performance will influence the ℓ_{xy} distribution. Figure 4 shows the ℓ_{xy} distributions of both prompt and B-decay J/ψ for perfect alignment and for the alignment expected with 10 pb^{-1} of data. The unbinned likelihood fit to obtain the fraction of J/ψ from B-hadron decays was repeated with the 10 pb^{-1} misalignment sample. The relative difference between the fitted B-hadron fractions for the two misalignment scenarios is about 4 %, aver-

Table 2: J/ψ mass resolution in different misalignment scenarios.

	10 pb^{-1}	100 pb^{-1}	ideal
J/ψ mass resolution (MeV/c^2)	34.2	30.5	29.5

aged over the full $p_T^{J/\psi}$ range.

7 Systematic uncertainties

A full estimation of all systematic uncertainties is only possible when actual collision data will be available. For example, tag and probe methods will be used to assess the systematic uncertainties on the reconstruction and trigger efficiencies coming from a non-perfect detector Monte Carlo simulation. Dedicated study groups will assess this uncertainty for CMS. Extrapolating from the CDF measurement [5], it is expected to be around 5%. Uncertainties in luminosity and momentum scale will also be evaluated by dedicated study groups and are expected to be 10% and 1%, respectively. The most important contributions to the systematic uncertainties are summarized in Table 3. The effects of these systematic uncertainties were evaluated in each $p_T^{J/\psi}$ bin.

Uncertainties due to the J/ψ invariant mass fit affect the number J/ψ events and were estimated by comparing a double Gaussian with a single Gaussian fit in three different $\eta^{J/\psi}$ regions for each $p_T^{J/\psi}$ bin. The uncertainty from the J/ψ polarization affects the acceptance (see Fig. 2) and was taken into account by shifting the polarization measured by CDF [6] (for prompt J/ψ's) and BaBar [13] (for non-prompt J/ψ) by $\pm$ 3 σ, a conservative but justified shift given the inconsistencies between CDF Run 1 and Run 2 measurements. Uncertainties arising from the B-hadron lifetime model were estimated by varying the shape of the non-prompt J/ψ ℓ_{xy} distribution in $F_B(\ell_{xy})$ in the unbinned maximum likelihood fit (see Eq. 4) and comparing the results. Uncertainties in the resolution function for prompt and non-prompt J/ψ's in Eq. (4) were taken into account by varying its shape in the likelihood fit. Uncertainties from the background description and normalisation, resulting for example from the level of the background due to two muons from pion or kaon decays, were taken into account by varying the background level conservatively by 50%. Uncertainties from misalignment in early data were assessed by comparing different misalignment scenarios.

8 Results and prospects

Table 4 displays the values of the J/ψ differential cross section with systematic and statistical uncertainties. Figure 5 displays the inclusive (left) and prompt (right) J/ψ differential cross sections, with combined systematic and statistical uncertainties, corresponding to an integrated luminosity of 3 pb^{-1}. Figure 6 shows the result of the fits to the fraction of J/ψ's from B-hadron decay in each bin of $p_T^{J/\psi}$.

The measurement of the differential J/ψ cross section is shown to be feasible already for an integrated luminosity of 3 pb^{-1}. The low background level and the excellent performance of the reconstruction permit us to measure the inclusive $p_T^{J/\psi}$ differential $J/\psi \rightarrow \mu^+\mu^-$ production cross section, and determine the fraction of J/ψ produced by B-hadron decays, in the $p_T^{J/\psi}$ range between 5 and 40 GeV/c. The precision of the result is limited by systematic uncertainties, and is around 15 %. Given the rather low integrated luminosity considered here, these

Table 3: Summary of systematic uncertainties in the J/ψ cross section measurement using CMS early data. All the uncertainties are $p_T^{J/\psi}$ dependent, except for the uncertainty from luminosity. The total uncertainty is about 13% in the region $p_T^{J/\psi}$ >20 GeV/c and around 19% in the lowest $p_T^{J/\psi}$ bin, 5-6 GeV/c.

Parameter affected	Source	$\Delta\sigma/\sigma$
Luminosity	Luminosity	$\sim$ 10 %
Number of J/ψ	J/ψ mass fit	1.0 - 6.3 %
Number of J/ψ	Momentum scale	$\sim$ 1 %
Total efficiency	J/ψ polarization	1.8 - 7.0%
Total efficiency	J/ψ p_T binning	0.1 - 10 %
Total efficiency	MC statistics	0.5 - 1.7 %
$\lambda_{reconstruction}$	Non-perfect detector simulation	$\sim$ 5 %
$\lambda_{trigger}$	Non-perfect detector simulation	$\sim$ 5 %
B fraction	ℓ_{xy} resolution model	0. - 1.9 %
B fraction	B-hadron lifetime model	0.01 - 0.05 %
B fraction	Background	0.1 - 3.0 %
B fraction	Misalignment	0.7 - 3.5 %
Total systematic uncertainty 13-19 %		

results are less precise than those published by CDF [4, 5] in the $p_T^{J/\psi}$ range common to both measurements, but CMS will probe the cross section beyond 20 GeV/c for the first time, as well as at a higher center of mass energy. Some of the systematics will, of course, benefit from the larger data set that will be collected with higher integrated luminosities. The uncertainties in the background level will be checked in data directly, by studying the same-sign muon pairs. They will be used to check the agreement between the data and the Monte Carlo simulation, in terms of yield and shape of the background distributions. The tag and probe methods will also be more accurate, since the invariant mass fit will be feasible in different $\eta^{J/\psi}$ regions, where the momentum resolution is expected to differ noticeably. Therefore, after a few months of LHC operation, the measurement presented in this note should be doable with a significantly improved precision.

9 Conclusion

In this note we have described a feasibility study for measuring the J/ψ production cross section in the di-muon channel with 3 pb^{-1} of data to be collected by the CMS detector. We have shown how to measure the inclusive J/ψ cross section, as well as the prompt and non-prompt components separately, by making use of the large B-hadron lifetime. The most important uncertainties affecting the measurement are systematic. With the precision reported here, we should be able to probe the different charmonium production models already with the first LHC data.

The measurement of the J/ψ production cross section is only the first step to understand the mechanisms of J/ψ hadro-production. In particular, with more data we will be able to directly measure the prompt J/ψ polarization.

References

[1] N. Brambilla et al. *CERN Yellow Report* **CERN-2005-005** (2005).

Table 4: The prompt and B-decay J/ψ differential cross sections as a function of $p_T^{J/\psi}$ with statistical and systematic uncertainties. The cross section in each $p_T^{J/\psi}$ bin is integrated over the $\eta^{J/\psi}$ range $|\eta^{J/\psi}| < 2.4$. The Monte Carlo input values are listed in the last 2 columns.

$p_T^{J/\psi}$ (GeV/c)	Fitted $d\sigma/dp_T \cdot Br$ (nb/GeV/c)		MC $d\sigma/dp_T \cdot Br$ (nb/GeV/c)	
	prompt J/ψ	B-decay J/ψ	prompt J/ψ	B-decay J/ψ
5-6	216±15($stat$)±42($syst$)	52.6±3.6($stat$)±10.1($syst$)	217	50.6
6-7	129±4±18	31.1±1.0±4.3	128	32.9
7-8	73.8±1.6±10.2	22.9±0.5±3.2	73.6	23.8
8-9	44.1±0.8±6.0	15.6±0.3±2.1	43.8	16.4
9-10	26.9±0.5±3.8	11.3±0.2±1.6	27.1	11.5
10-11	16.6±0.3±2.2	7.88±0.14±1.06	16.7	8.09
11-12	11.0±0.2±1.4	5.57±0.10±0.71	10.9	5.88
12-13	6.98±0.14±0.94	4.15±0.08±0.56	7.03	4.23
13-14	4.80±0.10±0.63	2.87±0.06±0.38	4.76	2.98
14-15	3.39±0.08±0.46	2.15±0.05±0.29	3.35	2.23
15-17	2.04±0.04±0.30	1.44±0.03±0.21	2.03	1.48
17-20	0.944±0.019±0.133	0.742±0.015±0.105	0.934	0.765
20-24	0.379±0.010±0.055	0.320±0.008±0.046	0.377	0.325
24-30	0.131±0.004±0.019	0.122±0.004±0.017	0.128	0.125
30-40	0.0348±0.0015±0.0052	0.0346±0.0015±0.0051	0.0333	0.0356

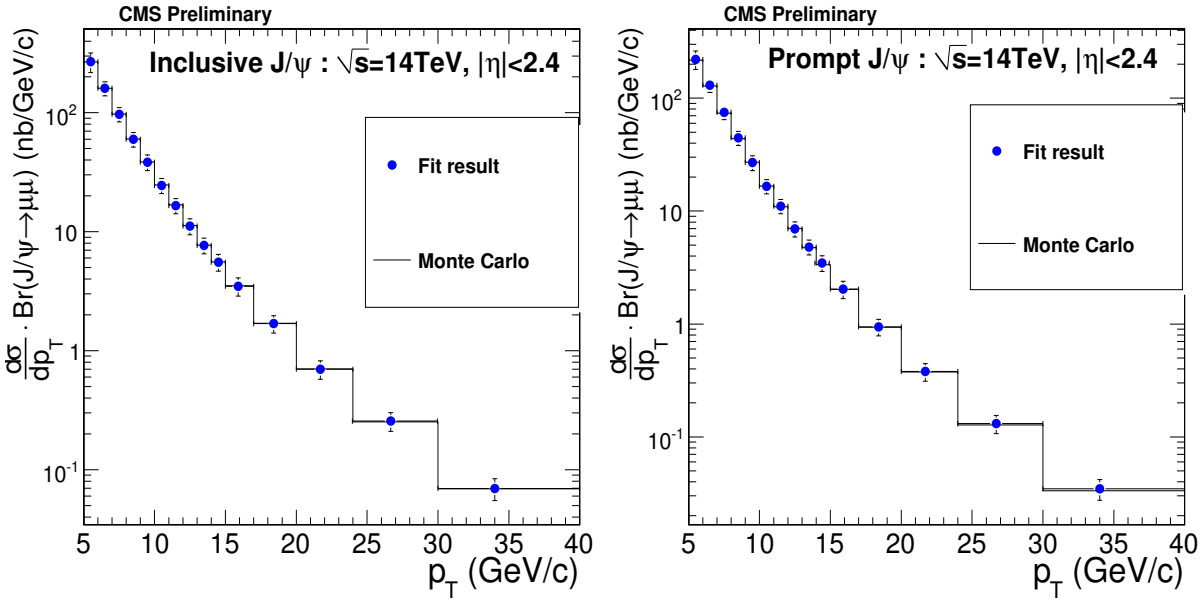

Figure 5: The inclusive (left) and prompt (right) J/ψ differential cross section, $d\sigma/dp_T \cdot Br(J/\psi \to \mu^+\mu^-)$, as a function of $p_T^{J/\psi}$, integrated over the pseudorapidity range $|\eta^{J/\psi}| < 2.4$, corresponding to an integrated luminosity of 3 pb^{-1}.

[2] J. Lansberg *Int. J. Mod. Phys. A* **21** (2006) 3857.

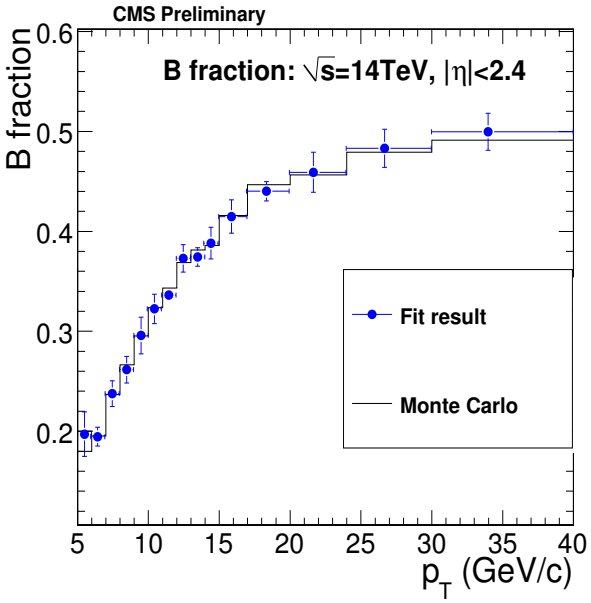

Figure 6: The fitted fraction of J/ψ's from B-hadron decays, as a function of $p_T^{J/\psi}$, integrated over the pseudorapidity range $|\eta^{J/\psi}| < 2.4$, corresponding to an integrated luminosity of 3 pb^{-1}.

[3] M. Krämer *Prog. Part. Nucl. Phys.* **47** (2001) 141.

[4] **CDF** Collaboration *Phys. Rev. Lett.* **79** (1997) 572.

[5] **CDF** Collaboration *Phys. Rev. D* **71** (2005) 032001.

[6] **CDF** Collaboration *Phys. Rev. Lett.* **99** (2007) 132001.

[7] **D0** Collaboration *Preliminary Result* **Conference Note 5089-CONF** (July 2007).

[8] T. Sjöstrand, S. Mrenna, and P. Skands *JHEP* **0605** (2006) 026.

[9] M. Bargiotti and V. Vagnoni *LHCb-2007-042* (2007).

[10] **CMS** Collaboration *The Trigger and Data Acquisition Project, Vol. II* **CERN/LHCC 2002-026**.

[11] **CMS** Collaboration *CMS Physics: Technical Design Report Volume 1* **CERN/LHCC 2006-001**.

[12] **CDF** Collaboration *Phys. G* **34** (2007) 2457.

[13] **BaBar** Collaboration *Phys. Rev. D* **67** (2003) 032002.